ELSEVIER

Journal of Applied Geophysics 49 (2002) 185–194

JOURNAL OF APPLIED GEOPHYSICS

www.elsevier.com/locate/jappgeo

Square array anisotropy measurements and resistivity sounding interpretation

M.J. Senos Matias

Department of Geosciences, University of Aveiro, 3800 Aveiro, Portugal

Received 21 December 2000; accepted 3 December 2001

Abstract

The use of geophysics in shallow investigations, such as in environmental, geotechnical and hydrogeological studies requires the development of fast, reliable, high-resolution field and interpretation techniques. When resistivity methods are used, limitations can be expected if ground inhomogeneities and anisotropy are present. In these cases, 1D surveys are not suitable and 2D approaches need geological information so that adequate survey line orientation is chosen. On the other-hand, 3D techniques could prove to be expensive and time-consuming, both in the field and at the interpretation stages. Non-conventional electrode arrays, such as the square array, have been proposed and could provide useful information on local inhomogeneities and anisotropy. However, interpretation material for these arrays is still difficult to obtain. In this paper, it will be shown how conventional resistivity sounding curves can be used to derive ground anisotropy parameters when square arrays are applied. At first, two-layer sounding model curves are interpreted with traditional 1D resistivity curves and estimates for the model apparent resistivity, anisotropy, and strike are derived. Then, several field curves for two, three and four layers are fully interpreted, and it is demonstrated how to obtain depths, apparent resistivity, strike and apparent anisotropy estimates for concealed earth layers.

Keywords: Resistivity; Anisotropy; Azimuth; Variation; Sounding; Interpretation; Square array

1. Introduction

It is well known that ground inhomogeneity and anisotropy can produce strong orientational effects in resistivity measurements and sounding curves. At first, to overcome this problem, it was proposed to conduct surveys using a favourable orientation with respect to the geological strike prevailing in the area and earth resistance measurements from perpendicular array orientations were used. Then, nonconventional arrays such as the square array, Habberjam (1979), were proposed as well as azimuthal resistivity measurements and diagrams (for instance Bolshakov, et al. (1995, 1998a,b); Almeida and Senos Matias (1991) and others). Generally speaking, these techniques consist of measuring earth resistance at several array orientations and plotting the data in a polar form to investigate subvertical faulting. When the polar diagram conforms to an ellipse, it is taken to represent anisotropy homogeneity. Several successful applications have been discussed and reported in the literature (Busby, 2000).

The square array and its modified version (Habberjam, 1979) have also proven to be very effective in

E-mail address: mmatias@geo.ua.pt (M.J. Senos Matias).

0926-9851/02/$ - see front matter
PII: S0926-9851(01)00113-6

the investigation of ground inhomogeneity and anisotropy, whose effects in these types of measurements have already been discussed (Senos Matias and Habberjam, 1984, 1986).

However, interpretation material for these arrays is difficult to obtain (Senos Matias, 1999), and the interpretation techniques for sounding curves over anisotropic ground are not common, although some numerical algorithms are available (Bolshakov et al., 1998b).

Therefore, to overcome such problems, herein, it will be shown how to use square array data and conventional 1D resistivity sounding curves to obtain estimates for the ground mean resistivity, apparent anisotropy and concealed strike. The use of square arrays also provides a fourth parameter, the "anisotropic noncompatibility ratio" (Habberjam, 1979), which is an indication of whether the subsurface is anisotropic or if fracturing or other inhomogeneities prevail.

To achieve these goals, data will be used from analogue modelling to establish interpretation procedures and guidelines. Afterwards, several field curves will be interpreted fully.

2. Orientational effects on resistivity sounding curves

Resistivity sounding curves can be affected by anisotropy. Fig. 1 shows the effect of bedrock anisotropy on sounding curves obtained with linear arrays oriented at right angles, where orientation A is parallel to the known geological strike, and orientation B is perpendicular to the geological strike. Thus, on the top of Fig. 1, the sounding curves correspond to an earth where gently dipping limestone beds are concealed by drift. In this case, it is clear that both curves A and B are nearly identical and conventional 1D modelling can be done.

On the other hand, the bottom of Fig. 1 shows the response over an earth consisting of a steeply dipping bedrock schist covered by drift. As can be seen from the figure, resistivity sounding curves vary significantly with orientation and 1D modelling will depend on the array orientation used. Therefore, prior knowledge of the general geological strike of concealed formations is needed.

Unfortunately, very often this information is not available and such orientational variation is ignored.

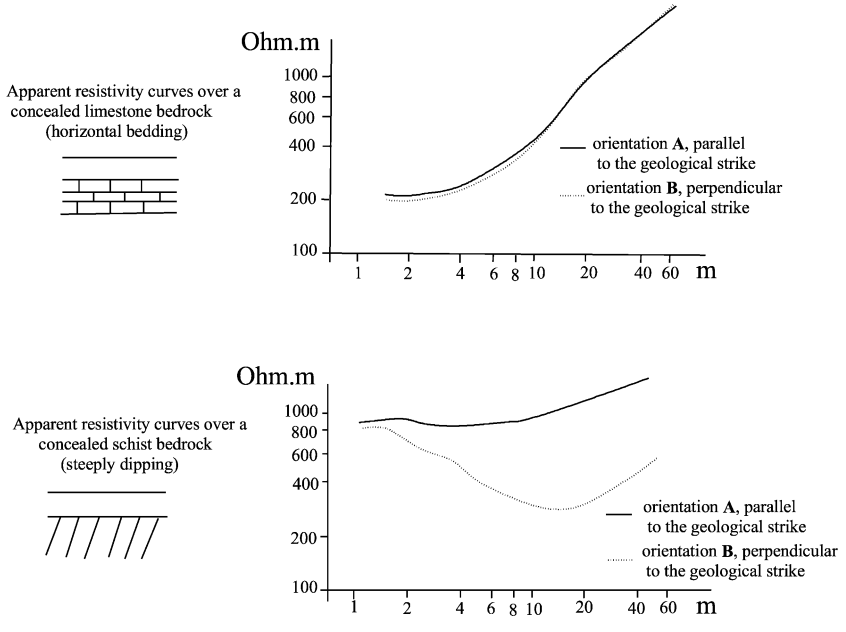

Fig. 1. Field resistivity sounding curves over a concealed, gently dipping bedrock (top) and a concealed, steeply dipping bedrock (bottom); (orientation A parallel to the strike, orientation B perpendicular to the strike).

While this may be reasonable in flat or gently dipping lying areas, in more complex regions, where steep dips can be encountered, such variations should not be ignored.

Field investigations and laboratory work (Senos Matias and Habberjam, 1984) have shown that, to a reasonable approximation, the observed orientational variation conforms closely to that obtained over a uniform anisotropy medium (Fig. 2).

Over such a medium, it is possible to define a mean resistivity, ρ_m, and the anisotropy coefficient, λ,

$$\rho_m = \sqrt{\rho_l \rho_t} \qquad \text{and} \qquad \lambda = \sqrt{\rho_l / \rho_t}.$$

Commonly, the anisotropy coefficient, λ, varies from one to two (Keller and Frischknecht, 1979), and it is not unusual to obtain values larger than 1.5 in areas where strong dips prevail. Over such an anisotropic model, the electrical potential V for a point P at a distance r from a current point C, is given by,

$$V = \frac{I\rho_m}{2\pi r}(1 + (\lambda^2 - 1)\sin^2\theta\sin^2\alpha)^{-1/2}.$$

The parameters λ and α cannot be separated but they can be combined such that (Habberjam, 1979),

$$n = (1 + (\lambda^2 - 1)\sin^2\alpha)^{-1/2}$$

where "n" is the so-called equivalent vertical anisotropy that varies from 1 to λ. Now the earth resistance R will be,

$$R = \frac{V}{I} = \frac{\rho_m}{2\pi r}(1 + (n^2 - 1)\sin^2\theta)^{-1/2}.$$

Thus, R varies from a minimum $\rho_m/(2\pi rn)$ for $\theta = 90°$ to a maximum $\rho_m/(2\pi r)$ for $\theta = 0°$. If such a model is to be investigated, it is necessary to obtain estimates for the values of ρ_m, "n" and the strike (that is the direction where the maximum earth resistance was measured). In others words, there is a need for sampling the earth at three different orientations to obtain such estimates.

The crossed square array provides four sampling orientations, and processing of the earth resistances allows the computation of estimates for the above parameters (Habberjam, 1975, 1979). Furthermore, as there is an extra orientation measured, it is possible to derive a fourth parameter, the "anisotropic noncompatibility ratio" (ANCR), which expresses the homogeneous anisotropic half space conformity to describe the field observations. This parameter is strongly dependent on orientation, but analysis of ANCR sections can be very useful in discriminating structures present in resistivity sections (Senos Matias, 1983).

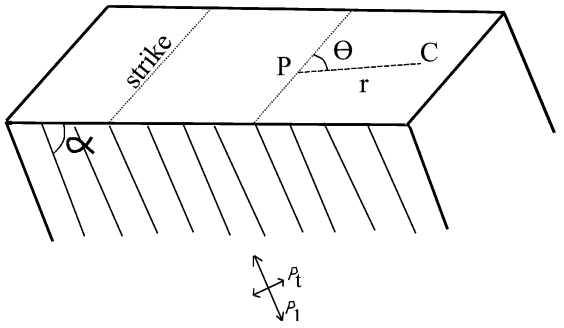

Fig. 2. Homogeneous anisotropic half space C is a current source, P the potential point, r the distance between them, θ the orientation of the two electrode CP array with respect to the geological strike and α is the dip of the geological formations.

It has been proven that the crossed square array shows extreme orientation responses at 0° and 22.5° to the strike (Habberjam, 1975). Furthermore, the crossed square array was proven to be orientationally stable, even in cases of severe anisotropy (Senos Matias and Habberjam, 1984, 1986). Therefore, this array could be used in most field situations without prior knowledge of the geological strike.

3. Two-layer model with an anisotropic basement

An automated tank analogue was used to obtain data over a two-layer model with a concealed anisotropic basement (Karwatowsky and Habberjam, 1981). This model was constructed by using an alternate sequence of vertical insulating PVC plates (0.6 cm thick) and brine. Thus, a severe resistivity contrast was expected between the PVC plates and the brine, which also formed the top layer. Two horizontal holes were drilled in the PVC plates to allow some current to flow perpendicular to the plates strike.

In Fig. 3, data are shown for depths of burial of 1.5 and 6 cm to the top of the brine surface, for a crossed square array expanding from a minimum square side

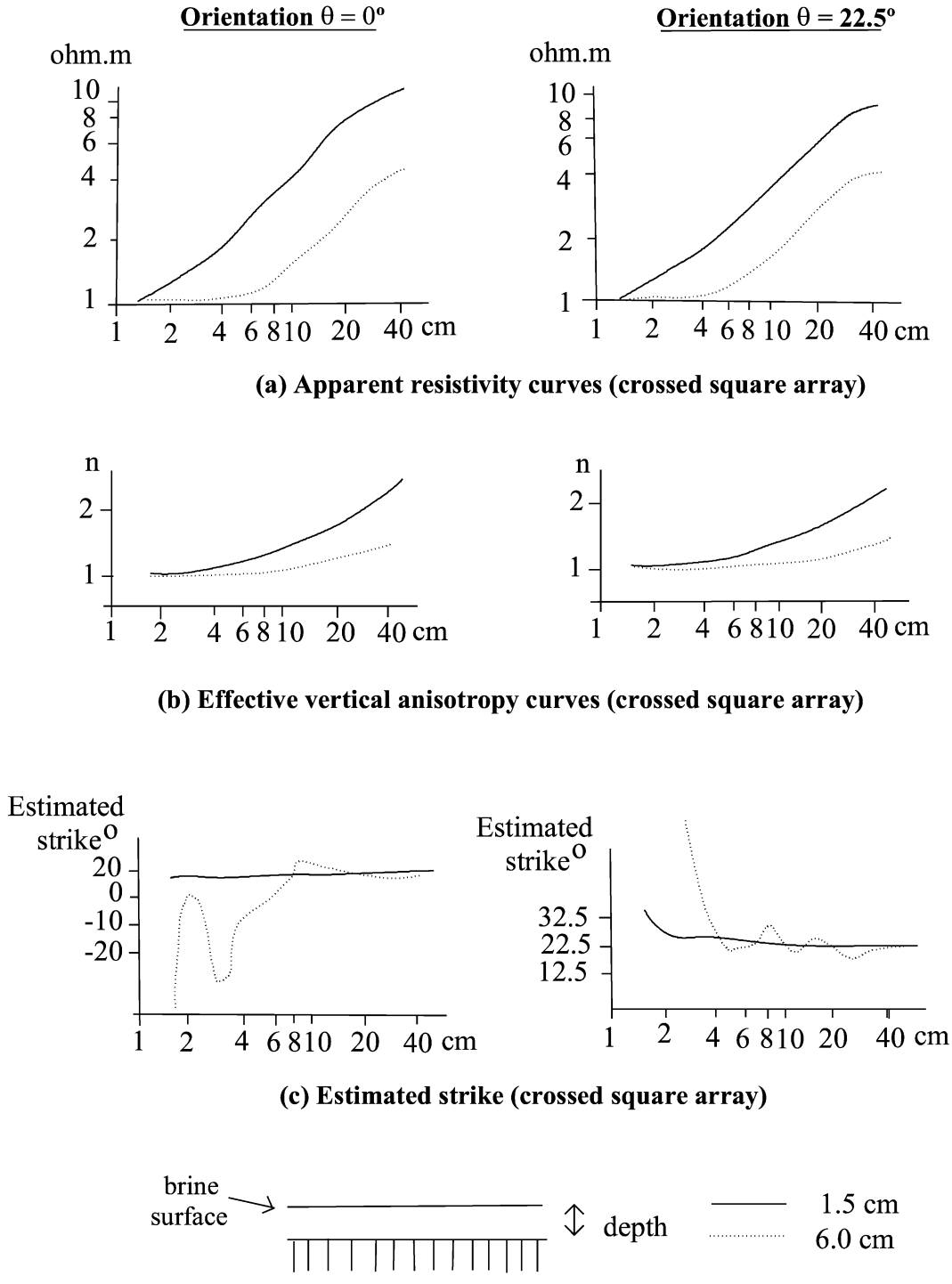

Fig. 3. Sounding curves for a concealed anisotropic basement model for crossed square array orientations of 0° and 22.5° to the model strike. (a) Apparent resistivity curves; (b) effective vertical anisotropy curves; (c) estimated strike curves.

Table 1
Estimated "n" and strike values for a two-layer model (anisotropic basement)

Spacing (cm)	Depth (1.5 cm)				Depth (6 cm)			
	Orientation (0°)		Orientation (22.5°)		Orientation (0°)		Orientation (22.5°)	
	"n"	θ	"n"	θ	"n"	θ	"n"	θ
1.41	1.02	179	1.03	34	1.04	22	1.05	70
2	1.05	180	1.05	24	1.04	174	1.01	154
2.83	1.09	178	1.09	22	1.02	145	1.03	165
4	1.16	179	1.17	23	1.01	169	1.03	21
5.66	1.26	179	1.28	22	1.03	171	1.05	20
8	1.38	180	1.39	23	1.05	0	1.07	28
11.31	1.56	0	1.54	21	1.11	2	1.11	21
16	1.71	0	1.71	21	1.18	0	1.20	22
22.63	2.01	179	1.86	20	1.35	177	1.24	18
32	2.21	179	2.19	22	1.45	177	1.38	20
45.25	2.51	0	2.31	22	1.45	178	1.46	23

of 1.41 to a maximum of 45.25 cm, and using the orientation extremes of 0° and 22.5° to the model strike. That is, the current electrode lines 1–4 (Habberjam, 1979) of the crossed square array is oriented at 0° and 22.5°, respectively, with relation to the direction of the vertical PVC sheets, "the geological strike," which forms the anisotropic basement.

The mean resistivity curves (top of Fig. 3) show the typical steep two-layer sounding curves. The "n" curves show increasing values, with no signs of flattening off, while at the bottom of the figure, the computed strike curves clearly reveal the orientation of the basement.

In Table 1, the computed "n" and strike values show that accurate strike determinations are possible for "n" values greater than 1.08, which occur for a spacing approximately twice the depth of burial.

Using the mean resistivity equation, and considering the case of vertical or near vertical layering, that is $n = \lambda$, values for ρ_1 can be computed. Therefore, Fig. 4 shows the longitudinal resistivity curves for both orientation extremes and depths of burial.

The interpretation of the mean and longitudinal resistivity curves using conventional 1D procedures and interactive software is shown in Table 2.

From these interpreted data, values of 32 Ω m, and 2.67 could be calculated, respectively for the transversal resistivity, ρ_t, and anisotropy λ for the basement. On the other hand, values of 0.9 and 1.02 Ω m could be computed, respectively, for the transversal resistivity and anisotropy of the cover. The computed basement anisotropy value looks overestimated, but it must be remembered that the effective vertical anisotropy "n" curves (center of Fig. 3) are still rising and

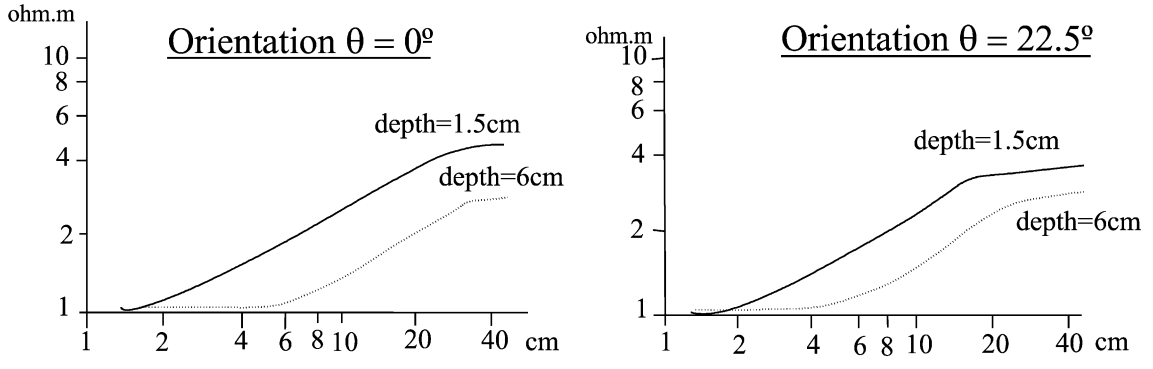

Fig. 4. Longitudinal resistivity curve.

Table 2
Interpretation parameters for the mean and longitudinal resistivity curves.

	Mean resistivity		Longitudinal resistivity	
	$\theta=0°$	$\theta=22.5°$	$\theta=0°$	$\theta=22.5°$
Depth (1.5 cm)				
Cover thickness (cm)	1.7	1.6	1.6	1.6
ρ_m Cover (Ω m)	0.85	0.85	0.8	0.8
ρ_m Basement (Ω m)	12	12	4.5	4.5
Depth (6 cm)				
Cover thickness (cm)	6	6	6	6
ρ_m Cover (Ω m)	0.9	0.95	0.9	0.9
ρ_m Basement (Ω m)	12	12	4.5	4.5

Model depths of 1.5 and 6 cm at the extreme array orientations.

thus show no sign of flattening off. Thus, if larger spacings were used, higher "*n*" values should have been recorded. Finally, the interpreted basement depths are in very good agreement with the model used and the isotropic character of the cover is confirmed as expected.

Thus, data provided from the use of crossed square arrays can be used to obtain estimates for all the parameters needed to describe anisotropic model layers, except for the inclination α. Moreover, estimates of the parameters for both orientation extremes are stable and so, it is not necessary to know the strike in order to conduct electrical soundings.

3.1. Field data

The crossed square array was used to carry out several resistivity soundings in Chapel-le-Dale, just to the North of Ingleton, in the Three Peaks Region, West Yorkshire Moors. The soundings were conducted in an area where schists and greywackes are concealed by drift at different depths and show an approximate NW–SE strike (Dunham et al., 1953).

The square array field orientation was such that the square diagonal, defined by electrodes 1–3 (Habberjam, 1979), is in the North–South direction, with electrode 1 to the North. Therefore, the square array lines 1–4, used to define the array orientation with respect to the strike, was in the NW–SE direction also. Thus, wherever anisotropy prevails, the strike estimates from field measurements should be zero for all the soundings.

4. Two-layer field curve CS1

4.1. Resistivity curves

On the left-hand side of Fig. 5, the mean resistivity field curve, ρ_m, shows a typical two-layer behaviour. On the same graph, the longitudinal resistivity curve, ρ_l, was obtained dividing the ρ_m values by the "*n*"

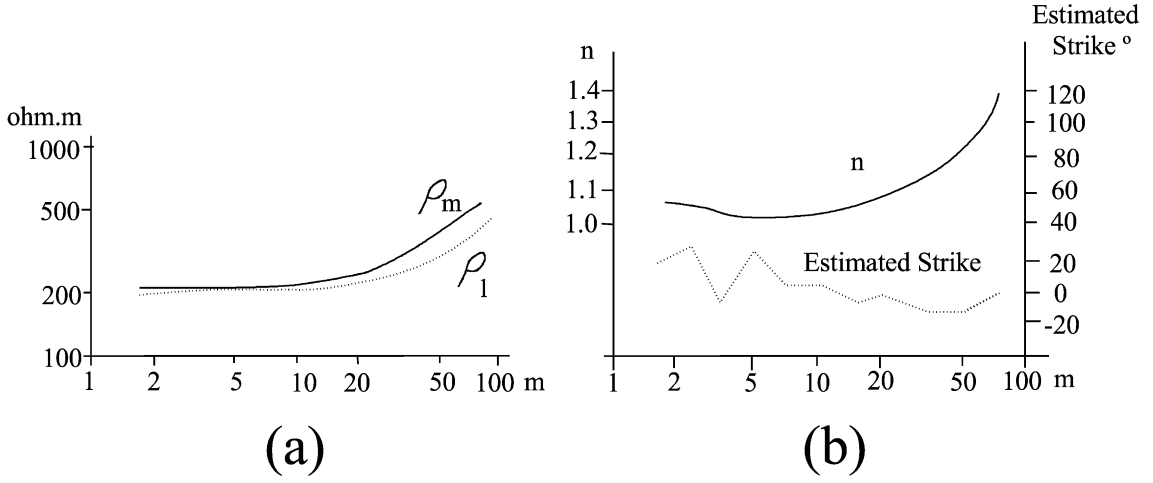

Fig. 5. Field curves for a two-layer case: (a) mean and longitudinal resistivity curves; (b) "*n*" and estimated strike curves.

Table 3
Interpretation parameters for the two-layer curve CS1

Using ρ_m			Using $\rho_l = \rho_m/n$		
Layer	ρ (Ω m)	Depth (m)	Layer	ρ (Ω m)	Depth (m)
1	225	18.9	1	216	18.7
2	1120	–		619	–
Misfit error, 1.2%			Misfit error, 2.3%		

values from the correspondent curve on the right. Similarly to the mean resistivity curve, the longitudinal resistivity curve is clearly a two-layer curve.

4.2. "n" Curve

On the right, the "*n*" curve shows a fairly constant behaviour for the shorter spacings. Thus, in this region, "*n*" values vary from 1 to 1.1 and should reflect the isotropic character of the drift. However, at larger spacings, that is greater than 32 m, "*n*" values rise and reveal an anisotropic basement. The "*n*" curve keeps rising and shows no signs of flattening off, that is, higher "*n*" values should be recorded if larger spacings were used.

5. Estimated strike curve

The estimated strike curve, at the right-hand side of Fig. 5, shows random values of θ for the shorter spacings, where low "*n*" values occur. Therefore, as expected, the drift does not show any orientational effects. On the other hand, for spacing values greater than 32 m, coherent strike values around zero are obtained and correspond to the increasing "*n*" values, confirming the anisotropic character of the second layer as well as the geological strike (Dunham et al., 1953).

Both the ρ_m and the ρ_l curves were interpreted using conventional 1D algorithms, bearing in mind the information from the "*n*" and estimated strike field curves, as well as previous model experience. Table 3 shows the interpretation parameters obtained.

From the above parameters, values of 1.04 and 1.81 could be estimated for the anisotropy of the first layer and for the anisotropic basement, respectively. On the other hand, values of 234 and 2026 Ω m could be obtained for the transversal resistivity of the cover and the basement, respectively. Finally, the computed strike, for spacing values greater than 1.1, is in close agreement with the geological strike in the region.

6. Three-layer field curve CS2

6.1. Resistivity curves

A three-layer field curve type H is shown in Fig. 6. The ρ_m curve corresponds to the field measurements, and the ρ_l curve was computed using the previous values and those of the "*n*" curve. Again, the longi-

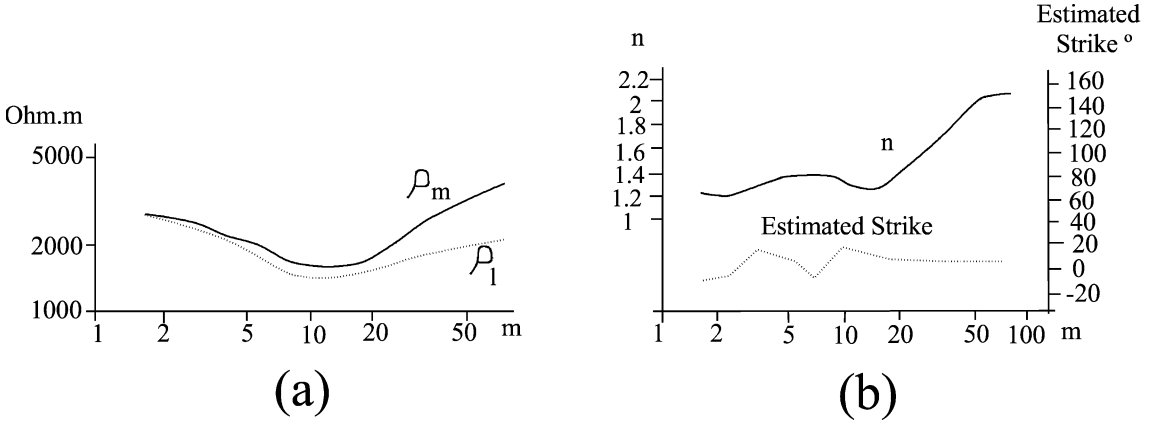

Fig. 6. Field curves for a three-layer case: (a) mean and longitudinal curves; (b) "*n*" and estimated strike curves.

Table 4
Interpretation parameters for the three-layer curve CS2

Using ρ_m			Using $\rho_l = \rho_m/n$		
Layer	ρ (Ω m)	Depth (m)	Layer	ρ (Ω m)	Depth (m)
1	2792	2.7	1	2297	2.4
2	741	6	2	698	6.1
3	3707	–	3	1652	–
Misfit error, 3.9%			Misfit error, 3.7%		

tudinal resistivity curve shows a similar shape to that of the mean resistivity curve.

6.2. "n" Curve

On the right-hand side of Fig. 6, the "*n*" field curve shows values of about 1.2 for spacing values less than 16 m. However, when spacing increases, "*n*" values increase sharply and values greater than 2 are registered. In this case, the "*n*" curve shows some signs of flattening off and therefore significantly higher "*n*" values for larger spacings should not be expected.

6.3. Estimated strike curve

This curve shows some variation for shorter spacings, that is for "*n*" values around 1.2. However, the observed variations are not as large as the ones recorded in the two-layer field curve. For a spacing larger than 16 m, coherent strike estimates, once again near zero, are obtained, confirming the anisotropic nature of the third layer. Moreover, the computed strike is in close agreement with the geological strike in this region (Dunham et al., 1953).

The interpretation of the resistivity curves was carried out as previously and the results are shown in Table 4.

From the parameters in Table 3, the values of 1.11, 1.06 and 2.24 can be estimated for the anisotropy of the three layers. On the other hand, values of 3394, 787 and 8318 Ω m are obtained for the transversal resistivities of the layers. Therefore, a highly anisotropic basement is diagnosed, and the computed "*n*" value is not far from that obtained from the flattening off value of the "*n*" field curve.

7. Four-layer field curve CS3

7.1. Resistivity curves

A four-layer field curve is shown in Fig. 7. The ρ_m and ρ_l curves, on the left part of Fig. 7, were constructed as in the previous cases, and have a similar shape.

7.2. "n" Curve

On the right-hand side of the figure, the "*n*" curve shows values less than 1.1 and a stable behaviour for

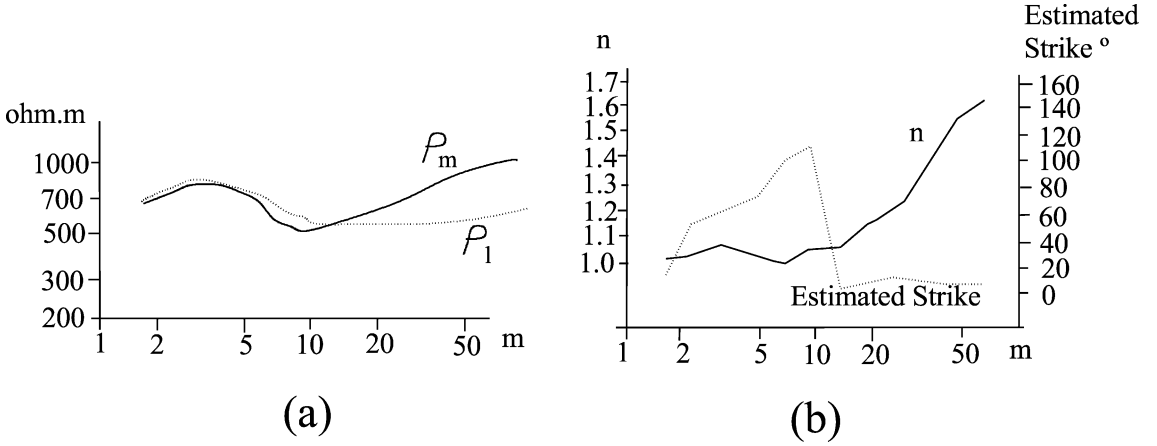

Fig. 7. Field curves for a four-layer case: (a) mean and longitudinal curves (b) "*n*" and estimated strike curves.

spacing values lower than 10. Thereafter, as spacing increases, "n" values increase sharply and the curve seems to be flattened off at values around 1.7. Therefore, it is expected that the last layer is severely anisotropic.

7.3. Estimated strike curve

The estimated strike curve shows erratic values for small spacings. This region of the curve also corresponds to low "n" values and thus no strike determinations are to be expected. However, for spacings greater than 10 and as "n" increases, the apparent strike determinations become stable, near zero, and in accordance with the general geological strike of the area (Dunham et al., 1953). Thus, the anisotropic character of the fourth layer is confirmed.

As in the previous cases, the mean and longitudinal resistivity curves have been interpreted using conventional 1D algorithms and incorporating the anisotropy information. The proposed interpretation is shown in Table 5.

From the parameters presented in Table 5, values of 1.02, 1.06, 0.7 and 1.8 can be estimated for the apparent anisotropy of the layers and values of 349, 2525, 150 and 2150 Ω m for the transversal resistivity of the layers. That is, the top two layers are isotropic. However, it must be noticed that at the third layer, apparent anisotropy is less than the unity. This means an anisotropy axes rotation, suggesting an oblate form of anisotropy ($n<1$). Such a behaviour has been observed before (Senos Matias and Habberjam, 1984), where high resistivity contrasts or strong structural effects rather than anisotropy are present. In the present case, the resistivity contrast between the third layer and the second and fourth layers is substantial, and therefore, if oblate anisotropy is present, it could have originated from this particular field situation.

Table 5
Interpretation parameters for the four-layer curve CS3

Using ρ_m			Using $\rho_l=\rho_m/n$		
Layer	ρ (Ω m)	Depth (m)	Layer	ρ (Ω m)	Depth (m)
1	342	0.5	1	335	0.5
2	2376	1.3	2	2235	1.2
3	219	4.5	3	320	4.5
4	1195	–	4	664	–
Misfit error, 2.8%			Misfit error, 2.09%		

The estimated strike curve, right-hand side of Fig. 7, gives very coherent strike values for spacings greater than 10 m. However, before this coherency is sustained, there is a small portion of the estimated strike curve with values rotated about 90° to the estimated strike. Therefore, the apparent strike curve also gives some indication of the presence of anisotropy axes rotation for the third layer.

8. Conclusions

The crossed square array provides very useful estimates for the mean resistivity, apparent anisotropy and strike for concealed anisotropic formations of the tank analogue experiments.

If the data are orientationally stable, there is no need for prior knowledge of the geological strike, and field observations could be conducted at any desired array orientation.

It is possible to carry out 1D interpretation using conventional resistivity sounding curves and software, if all the available information is used, that is the estimates for ρ_m, ρ_l, n and θ.

From the model studies, it was demonstrated that strike estimates are possible and accurate when "n" values are greater than 1.08. However, in field observations, it seems necessary to reach "n" values greater than 1.1.

The spacing for which that threshold is reached provides a good estimate for the depth of anisotropic formations, which is about 50% of that value. Therefore, the ambiguity and equivalence in data modelling can be reduced largely.

From the interpretation of different field curves, it is possible to estimate values for the mean, longitudinal and transversal resistivities, as well as depth, apparent anisotropy, and strike of concealed formations.

If a complete study is to be conducted over anisotropic ground, the crossed square array is the more economic field strategy, as the alternative is to carry out linear soundings in at least four different orientations. However, major disadvantages occur in rough and densely vegetated ground.

Finally, crossed square array field operations can be optimised easily by using multicables, multielectrode systems, appropriate switching boxes and PC control of field operations as in any other array.

References

Almeida, F., Senos Matias, M.J., 1991. A study of the orientational variation of induced polarization time domain data. 51st EAGE Conference, Florence, Italy. Extended Abstracts, pp. 360–361.

Bolshakov, D.K., Modin, I.N., Pervago, E.V., Shevnin, V.A., 1995. Anisotropy effects investigations by resistivity methods in some inhomogeneous media. 57th EAGE Conference, Glasgow, UK. Extended Abstracts, p. P034.

Bolshakov, D.K., Modin, I.N., Pervago, E.V., Shevnin, V.A., 1998a. New step in anistropy studies: arrow-type arrays. Proceedings of the 4th EEGS–European Section Meeting, Barcelona, Spain, pp. 857–860.

Bolshakov, D.K., Modin, I.N., Pervago, E.V., Shevnin, V.A., 1998b. Modeling and interpretation of azimuthal resistivity sounding over two layered model with arbitrary oriented anisotropy in each layer. Proceedings of the EAGE 60th Conference, Leipzig, Germany, p. P110.

Busby, J.P., 2000. The effectiveness of azimuthal apparent resistivity measurements as a method for determining fracture strike orientations. Geophysical Prospecting 48, 677–698.

Dunham, K.C., Hemmingway, J.E., Versey, H.C., Wilcockson, H.W., 1953. A guide to the geology of the district round Ingleborough. Proceedings of the Yorkshire Geological Society, vol. 29, pp. 77–115, part 2, No. 6.

Habberjam, G.M., 1975. Apparent resistivity, anisotropy and strike measurements. Geophysical Prospecting 23, 211–247.

Habberjam, G.M., 1979. Apparent resistivity observations and the use of square array techniques. Geoexploration Monographs No. 9. Geopublication Associate, Berlin.

Karwatowsky, J., Habberjam, G.M., 1981. A tunnel resolution investigation using an automated tank analogue. Geophysical Prospecting 29, 891–905.

Keller, G.V., Frischknecht, F.C., 1979. Electrical Methods in Geophysical Prospecting. Pergamon Press, New York, 523 pp.

Senos Matias, M.J., 1983. The use of field anisotropy measurements in resistivity field investigations. PhD Thesis, University of Leeds, Leeds, 297 pp.

Senos Matias, M.J., 1999. Electrical anisotropy parameters and resistivity sounding interpretation. Proceedings of the 5th EEGS–European Section Meeting, Budapest, Hungary, pp. Em9–EM10.

Senos Matias, M.J., Habberjam, G., 1984. A field example of the use of anisotropic parameters derived from resistivity soundings. Geophysical Prospecting 32, 725–739.

Senos Matias, M.J., Habberjam, G., 1986. The effect of structure and anisotropy on resistivity measurements. Geophysics 51, 964–971.